Ontario

Ministry of Transportation
Provincial Highways Management Division Report
Highway Infrastructure Innovation Funding Program

Acceptance Criteria for Ultrasonic Impact Treatment (UIT)

Final Report

February 2013

HIIFP-110

Technical Report Documentation Page

Publication Title	# Acceptance Criteria for Ultrasonic Impact Treatment (UIT)
Author(s)	Rana Tehrani Yekta, Dr. Scott Walbridge University of Waterloo
Originating Office	Bridge Office, Ontario Ministry of Transportation
Report Number	HIIFP-110
Publication Date	February 2013
Ministry Contact	Bridge Office, Ontario Ministry of Transportation 301 St. Paul Street, St. Catharines, Ontario, Canada L2R 7R3
Abstract	This study was undertaken to examine the fatigue performance of structural steel welds subjected to Ultrasonic Impact Treatment (UIT) at various levels, and to relate this performance to geometric and metallurgical properties measured to control the treatment quality. Fatigue tests of non-load carrying fillet welded attachments were conducted. Statistical analyses of the fatigue life data were performed and crack growth was monitored using the alternating current potential drop (ACPD) method. Measurement of local properties and examination of the weld toe microstructure were also performed. Lastly, the effects of weld toe geometry on the local stress concentration factors (SCFs) at various depths were investigated by finite element (FE) analysis. UIT significantly improved the fatigue lives of weld details regardless of the treatment level over the investigated range. The design fatigue lives of properly treated weld details were seen to increase by 274% to 962% at ΔS = 200 MPa. The treatment level had little impact on the mean S-N curves. However, it was seen to impact the design (i.e. 95% survival probability) S-N curves. Local near-surface microhardness and compressive residual stress measurements were greatest for the over-treated welds, followed by the properly treated and then the under-treated welds. Increasing the treatment speed resulted in a greater reduction in the surface microhardness and compressive residual stress levels than under-treating by decreasing the treatment intensity. The FE analysis showed that changes in weld toe geometry due to UIT can cause a decrease in the local SCFs. The SCF at the surface was the lowest for the properly treated welds and slightly higher for the under-treated welds. For the over-treated welds, the SCFs at the surface were nearly as high as for the untreated welds. The SCF increases as the thickness of the loaded plate increases up to T = 38 mm. With a further plate thickness increase, the SCF did not change substantially.
Key Words	Steel bridge welds; ultrasonic impact treatment; fatigue retrofitting; quality control
Distribution	Unrestricted technical audience.

Ontario

Ministry of Transportation
Highway Standards Branch Report

HIIFP-110

Acceptance Criteria for Ultrasonic Impact Treatment (UIT)

February 2013

Prepared by
Rana Tehrani Yekta and Dr. Scott Walbridge
University of Waterloo

Department of Civil and Environmental Engineering
200 University Avenue West
Waterloo, Ontario, Canada N2L 3G1

Table of Contents

Introduction

OVERVIEW

There are a number of possible approaches for dealing with fatigue problems in bridges, including: load restrictions, increased inspection frequency, member reinforcement, and member replacement. In certain situations, drilling a hole at the crack tip or "softening" the critical fatigue detail so that it attracts less load are also possibilities. Another possibility is the use of post-weld treatments (PWTs). PWTs can be divided into two categories: geometry improvement and residual stress-based methods. Hammer peening, needle peening, and ultrasonic impact treatment (UIT, see Figure 1) fall in the second category. With these methods, the objective is to eliminate tensile stresses and introduce compressive residual stresses by plastically deforming the weld toe, in order to slow or stop the propagation of fatigue cracks.

Highway authorities, such as the Ministry of Transportation of Ontario (MTO) have been seeking ways to improve the fatigue performance of their bridges. UIT represents a promising and relatively new approach for achieving this objective. The effectiveness of UIT is well documented through research, e.g. by [Haagensen et al., 1998], [Vilhauer et al., 2012] and [Nyborg et al., 2006]. However, there are a few challenges related to this treatment method that have slowed its adoption by bridge authorities. The most important of these is the lack of quality control procedures for accepting or rejecting the treatment once the work is completed. The effects on fatigue life of under-treatment and over-treatment are also uncertain.

Figure 1 – Ultrasonic Impact Treatment Equipment

RECENT RESEARCH ON UIT

As discussed in [Roy et al. 2003], UIT was first developed in the former U.S.S.R. to improve the fatigue performance of submarine hulls. UIT is similar to conventional needle or hammer peening in many respects. An important difference is that rather than using a pneumatic tool, which causes the needles or a single hammer-like rod to impact the weld surface at a frequency of 25-100 Hz, with UIT, the weld is impacted by a small number of rods vibrating at a much higher frequency on the order of 18000-27000 Hz. UIT offers a number of advantages over conventional peening. First and foremost, it is a much quieter device, which vibrates at a lower intensity, so that an operator can use it for longer periods of time before tiring.

A number of test-based studies of UIT have been reported recently in the literature. Recent research performed at Lehigh University is reported in: [Cheng et al. 2003, Roy et al. 2003, Roy 2006]. Tests of fatigue details on large-scale girder specimens are reported in [Roy et al. 2003, Roy 2006]. Based on the results of these tests, it is proposed that the detail category for certain UIT treated details be increased by ~one level (i.e. Det. Cat. 'C' up to 'B' for transverse stiffener welds). Testing at the University of Stuttgart on UIT for application to new high strength steel structures is summarized in: [Gunther et al. 2005, Kuhlmann et al. 2006]. These studies have focused on constant amplitude loading at positive R-ratios. A study from the Technical University of Braunschweig is reported in [Ummenhofer et al. 2006]. This appears to be the first study to examine the application of UIT under load.

A number of recommendations and codes have started to recognize the beneficial effects of residual stress-based PWTs on fatigue performance. The IIW [Haagensen and Maddox 2000] allows a vertical shift of the design S-N curve for needle and hammer peened welds. Specifically, this recommendation allows a 1.3-1.6 times fatigue strength increase, up to a treated fatigue strength of 100 MPa (at $N = 2 \cdot 10^6$ cycles). In Canada, the CSA Structural Welding Code [CSA 2003] allows a similar benefit for hammer peening, with the upper limit taken as the fatigue strength of the highest as-welded detail category. Other recommendations and codes containing similar provisions include: [DNV 2001] and [AWS 2004].

Guidelines for needle and hammer peening have also been developed by the IIW [Haagensen and Maddox 2000], including recommendations on the treatment speed, number of passes, air pressure provided to the pneumatic peening tool, etc. This reference also contains guidelines for operator training and quality control (after treatment) for conventional peening. These guidelines are limited, however, to qualitative means (e.g. visual inspection). [CSA 2003] includes rules regarding the depth of the groove due to hammer peening (0.5, 0.25, and 0.1 mm for low, medium, and high strength steel). This code also stipulates that the welds be inspected by magnetic particle or dye penetrant testing prior to peening.

The AASHTO Bridge Construction Specification [AASHTO 2008a] was recently updated with new clauses regarding the use of UIT on bridges. This standard recommends ("as a guide, not a requirement") a final indent depth due to UIT falling within the range of 0.25-0.5 mm. An ideal notch radius of 3 mm is recommended. Additional guidelines concerning the treatment application and qualitative quality control are also provided in this reference.

RESEARCH NEEDS

Despite the considerable body of research that has recently been published on UIT, a number of questions remain unanswered. Importantly among these, although guidelines for the evaluation of treatment quality now exist, it appears that they have been established primarily based on "best practices", and without any systematic investigation of the effects of under- or over-treatment on the fatigue performance increase due to UIT. This approach has left infrastructure owners such as highway authorities with questions that the previous research doesn't answer, such as: what are the consequences of small deviations from the quality control guidelines on the effectiveness of UIT? Can over-treatment result in repairable damage? And: can improper treatment actually lead to reductions in fatigue performance?

OBJECTIVES

Against this background, the objectives of the current study were as follows:

1. to examine the fatigue performance of structural steel welds subjected to UIT at various levels, including intentional under-treatment and over-treatment,

2. to relate the fatigue performance of the treated welds to geometric and metallurgical properties that can be measured to control the treatment quality, and

3. to use the results of the research conducted to achieve Objectives 1) and 2) to make recommendations for the quality control of UIT in bridge applications.

SCOPE

For this study, 42 weld specimens were fatigue tested in the University of Waterloo Structures Laboratory. The research was limited to the investigation of a single weld detail, specifically a non-load carrying fillet welded attachment, fabricated from CSA G40.21 350W steel. This detail falls under Detail Category 'C' according to the Canadian Highway Bridge Design Code (CAN/CSA S6-06). The fatigue tests were conducted under constant amplitude loading with and without under-loads at frequencies not exceeding 23 Hz.

The effectiveness of UIT in increasing the fatigue performance of the welds was evaluated through a variety of methods, including: fatigue testing, crack growth monitoring using the alternating current potential drop (ACPD) method, measurement of local properties (such as weld toe geometry, local hardness, and residual stresses), and an examination of the weld toe microstructure for untreated and treated welds. The effects of weld toe geometry on the local stresses in the untreated and treated welds were also investigated using elastic finite element (FE) analysis. All of the work carried out within the scope of this study was performed at the University of Waterloo, with the exception of the specimen treatment, which was performed by Applied Ultrasonics, and the residual stress measurements, which were performed by Proto Manufacturing, an external laboratory specializing in laser x-ray diffraction.

Experimental Program

The specimens were fabricated from 300 mm wide plates of CSA G40.21 350W steel with a thickness of T = 9.5 mm (3/8”). The transverse stiffeners were welded to the plates with four identical fillet welds using the flux-cored arc welding (FCAW) process. Following the welding, the 300 mm wide stiffened plates were saw cut into 50 mm wide strips. The ends were discarded to ensure that there were not any weld starts or stops within the specimen widths. The specimens were then treated by UIT using procedures and settings specified by the tool manufacturer, modified as specified in the test matrix (see Table 1). Following the treatment, the specimens were “dog-boned” using a computer numerical control (CNC) cutting machine.

The main reason for dog-boning the specimens is that during a previous test series, post-weld treatment by needle peening was seen to be so effective in some cases that cracks initiated in the gripped ends of the specimens rather than the weld toe [Ghahremani, 2010]. A second reason is that this ensured that there were no UIT starts or stops within the tested specimen width. The geometry of the dog-boned specimens is shown in Figure 2.

Table 1 – Test Matrix.

					ΔS (MPa)			
Group	Treatment	Timing	Method	Loading	200	225	250	
A	Untreated	N/A	N/A	CA	A1	A2	A3	Specimen I.D.
				CA-UL	A4	A5	A6	
B	Under-Treated (Reduced Intensity)	Before Cycling	Robotic	CA	B1	B2	B3	
				CA-UL	B4	B5	B6	
C	Under-Treated (Increased Speed)	Before Cycling	Robotic	CA	C1	C2	C3	
				CA-UL	C4	C5	C6	
D	Over-Treated	Before Cycling	Robotic	CA	D1	D2	D3	
				CA-UL	D4	D5	D6	
E	Properly Treated	Before Cycling	Robotic	CA	E1	E2	E3	
				CA-UL	E4	E5	E6	
F	Properly Treated	Before Cycling	Manual	CA	F1	F2	F3	
				CA-UL	F4	F5	F6	
G	Properly Treated	After Pre-Cracking	Manual	CA	G1	G2	G3	
				CA-UL	G4	G5	G6	

Two stress history types were investigated in this study: constant amplitude (CA) loading and constant amplitude loading with periodic under-load cycles (CA-UL). Figure 3 shows samples of each loading history type. Even though real loading histories in bridges tend to vary in amplitude, CA loading tests are commonly used to characterize the fatigue performance of welds. Compressive under-load cycles are known to be particularly severe for welds improved using residual stress-based post-weld treatments such as UIT.

For each specimen, the cycling was continued until failure or until a large N (3 to 9 million cycles) was reached without failure, in which case the test was considered to be a "run-out". For the CA loading, specimens were tested at stress ranges of 200, 225, and 250 MPa. A stress ratio (S_{min} / S_{max}) of R = 0.1 was used for all tests. For the CA-UL loading, 1000 cycle blocks were repeated through the duration of the test. Of these, ten cycles were compressive under-load cycles with stress ranges of 440, 500, and 556 MPa and a stress ratio of R = -1. The other 990 cycles had stress ranges of 200, 225, and 250 MPa and a stress ratio of R = 0.1, similarly to the CA loading history. For plotting the data for the CA-UL loading tests, an equivalent stress range was calculated using Miner's sum and an assumed S-N curve slope of m = 3.

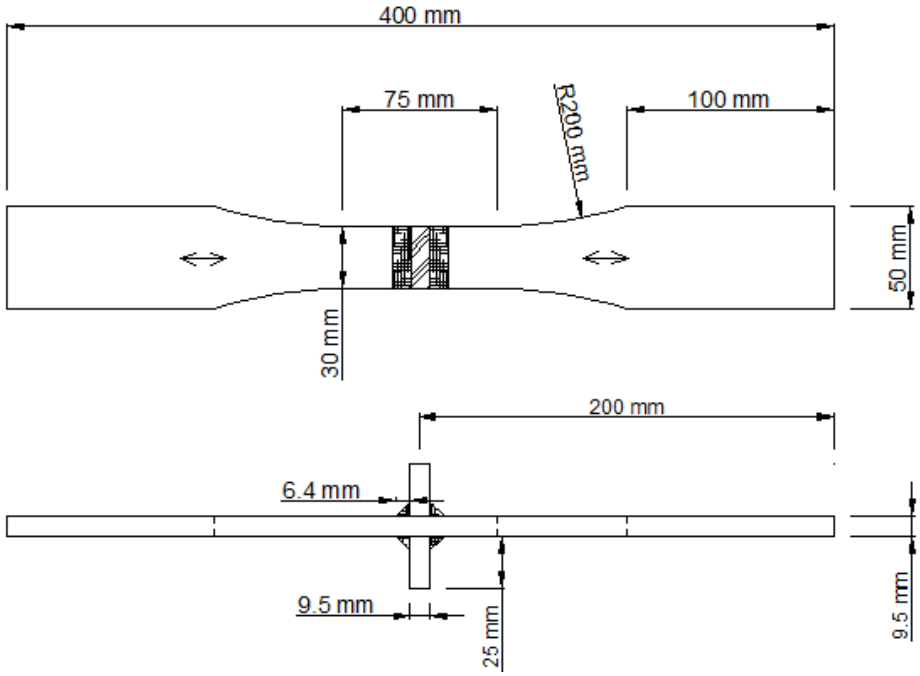

Figure 2 – Transverse Specimen Geometry after Dog-Boning

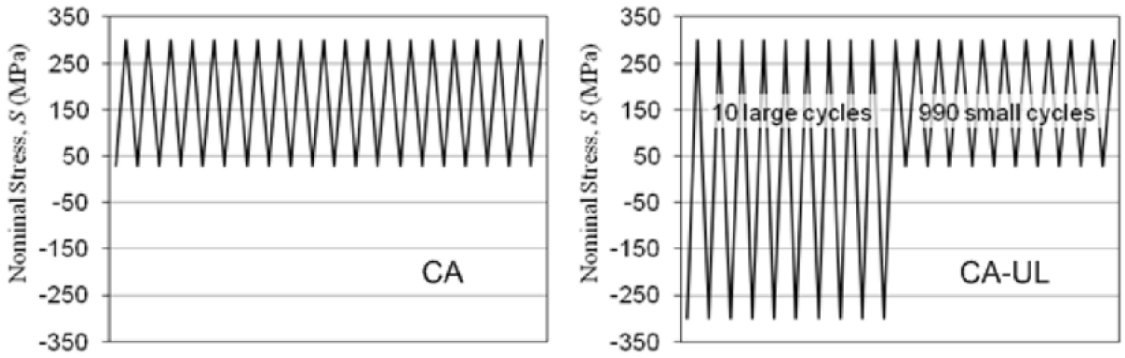

Figure 3 – CA and CA-UL Fatigue Loading Histories

In the current study, treatment level or "quality" was varied intentionally. Under-, over-, and properly treated specimens were tested. The under-treated specimens were tested to determine whether a fatigue life increase still occurs if the magnitude of the compressive residual stresses

is reduced. The over-treated specimens were tested to determine whether over-treating results in significant damage to the weld. Of these two scenarios, bridge owners are generally more concerned about over-treatment, since this problem is less easy to correct. The treatments were performed either manually or using a robot. The robot was programmed to perform the treatment at various settings to simulate under-, over-, and proper treatment. Although UIT is performed manually on actual bridges, it was thought that the use of the robot for simulating the various levels of treatment quality would lead to reduced variability and bias in parameters such as the treatment speed and duration. Proper treatment was assumed to correspond with a treatment speed of 10 mm/s and amplitude of 27-29 μm. Two kinds of under-treatment were considered: under-treatment by reducing the intensity or amplitude (from 27-29 μm down to 18 μm) and by increasing the treatment speed (from 10 to 20 mm/s). Over-treatment was simulated by reducing the treatment speed from 10 mm/s to 1 mm/s. This results in a large increase in the number of impacts of the UIT pins per mm of weld. The chosen speed over-treatment speed was thought to be an extreme lower bound for unintentional over-treatment. In all cases, the treatment was carried out in four "passes" at angles of 45º, 30º, 60º, and 45º.

Figure 4 shows a specimen after over-treatment using the robot. In the case of over-treatment to this extent, significant flaking of the weld toe material was apparent afterwards, as can be seen in this figure. The presence of such flaking could be used as a means of quality control, if a weld inspector is present while the treatment is being performed.

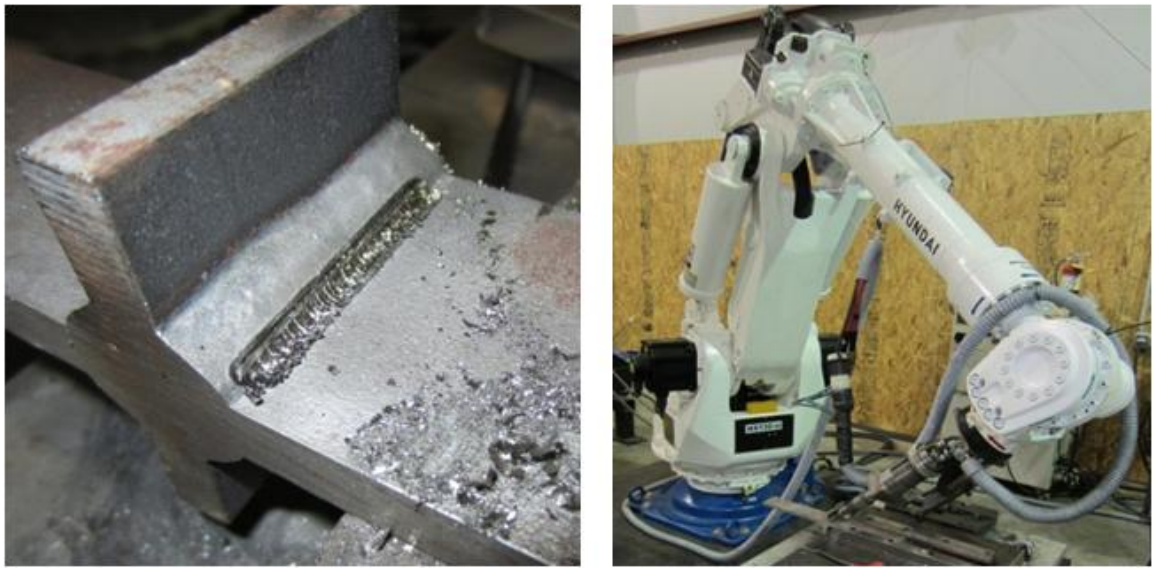

Figure 4 – Over-Treated Specimen (Left), and Robot (Right)

Figure 5 shows three weld toes subjected to under-, over-, and proper treatment. Looking at this figure, it can be seen that the properly treated groove is uniform, smooth, and centred on the weld toe. The over-treated groove is rough and flaking. The under-treated groove has a visible line at the centre corresponding with the location of the original weld toe.

The alternating Current Potential Drop (ACPD) technique was used on all of the specimens during the fatigue tests to monitor the crack sizing and crack growth. According to this

technique, an alternating current is caused to flow between field probes and then the voltage drop between voltage probes is measured [Costa Borges, 2008]. The ACPD system used in this research consisted of a custom-made, magnetic two site ACPD array, TSC ACPD Mk IV instrument, and LIMOS data acquisition software [Lugg, 2008].

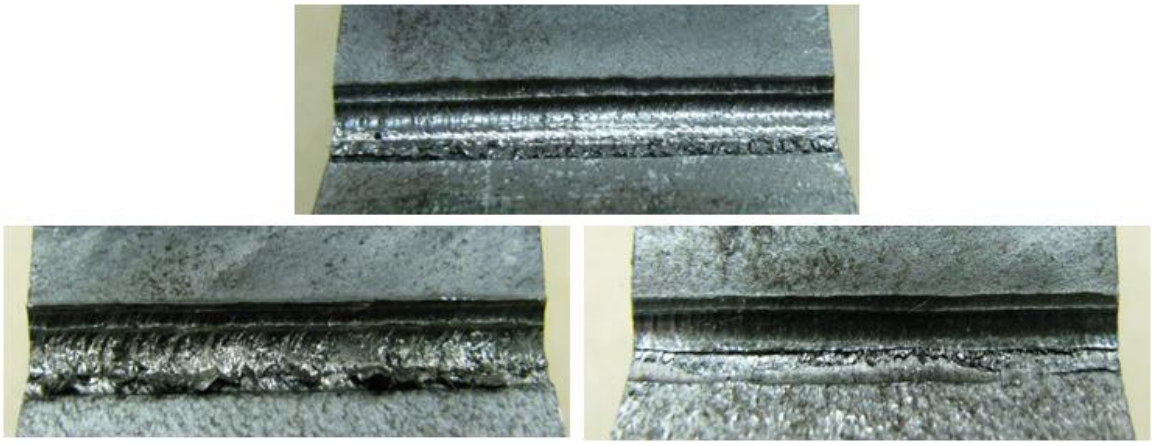

Figure 5 – Properly Treated (Group E, Top), Over-Treated (Group D, Bottom Left), and Under-Treated (Group B, Bottom Right)

Before using the ACPD arrays, the specimens were sandblasted to remove mill scale that might interfere with the electrical current. A thin strip of tape was placed on the weld toe before sandblasting to protect it, so that the sand blasting would not influence the test results. Four arrays were used for each test. Each array was connected to one of the four critical weld toes. Figure 6 shows the ACPD arrays attached to a fatigue specimen.

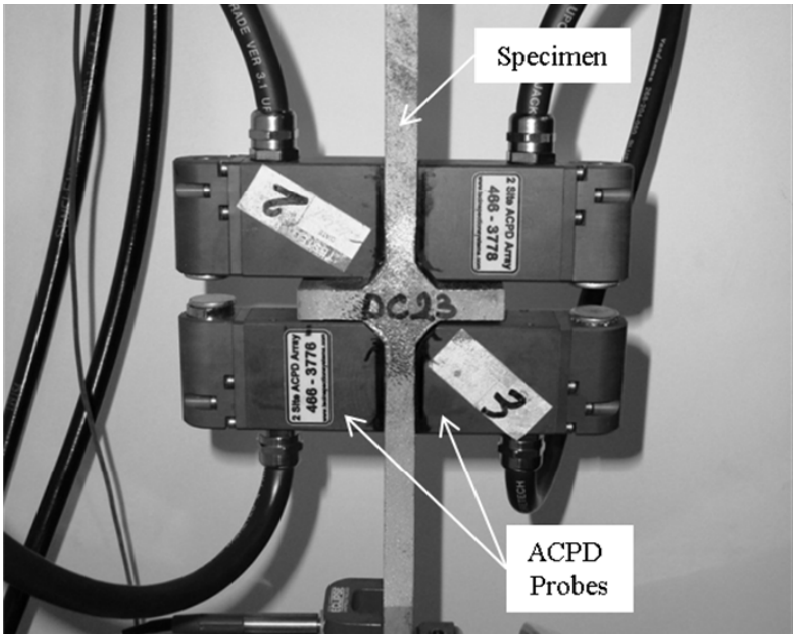

Figure 6 – ACPD Probes on the Specimen during Testing

Experimental Results

Tables 2 and 3 show the number of cycles to failure, *N*, for each tested specimen. The specimens that are in underlined are "run-outs" and did not experience fatigue failures.

Table 2 – Fatigue Lives of Group A, B, C, and D Specimens.

Specimen	*N*	Specimen	*N*	Specimen	*N*	Specimen	*N*
A1	248,383	B1	2,099,320	C1	1,537,837	D1	3,436,785
A2	166,821	B2	3,510,188	C2	8,210,202	D2	1,932,685
A3	105,487	B3	1,773,851	C3	3,031,499	D3	450,647
A4	202,874	B4	3,667,264	C4	3,564,413	D4	2,649,012
A5	185,887	B5	4,159,128	C5	4,796,216	D5	876,309
A6	94,746	B6	816,298	C6	460,835	D6	485,965

Table 3 – Fatigue Lives of Group E, F, and G Specimens.

Specimen	*N*	Specimen	*N*	Specimen	*N*
E1	3,021,835	F1	7,692,074	G1	5,598,137
E2	2,244,137	F2	4,207,209	G2	5,600,000
E3	2,753,812	F3	1,175,500	G3	2,143,443
E4	8,873,089	F4	3,141,363	G4	397,261
E5	2,064,805	F5	1,938,919	G5	357,136
E6	533,901	F6	561,878	G6	1,495,138

Stress-life (S-N) results for the various specimen groups are plotted in Figures 7 and 8. In the graphs in these figures, the untreated specimens under CA loading and CA-UL are shown with black and grey hollow symbols respectively. The treated specimens under CA loading and CA-UL are shown with filled black and grey symbols respectively.

Figure 7 shows the S-N data for Groups A, E, and F (untreated and properly treated specimens). The Detail Category 'C' design curve in this figure corresponds with a 97.7% survival probability [AASHTO 2008b, CAN/CSA S6-06]. It can be observed that all of the data points are above this curve. The fatigue lives of the untreated Group A specimens are closer to the Detail Category 'C' line whereas, the fatigue lives of the Group F specimens (properly, manually treated) are shifted considerably to the right and hence it can be concluded that there is an improvement in fatigue performance as a result of the treatment.

Group F had two run-outs, which are shown with an arrow on top of the symbol. As also seen in this figure, the results from Group E and F (properly, robotically treated) fall more-or-less on

top of each other, which means there is little difference between the manually and robotically treated specimens from the point of view of fatigue performance.

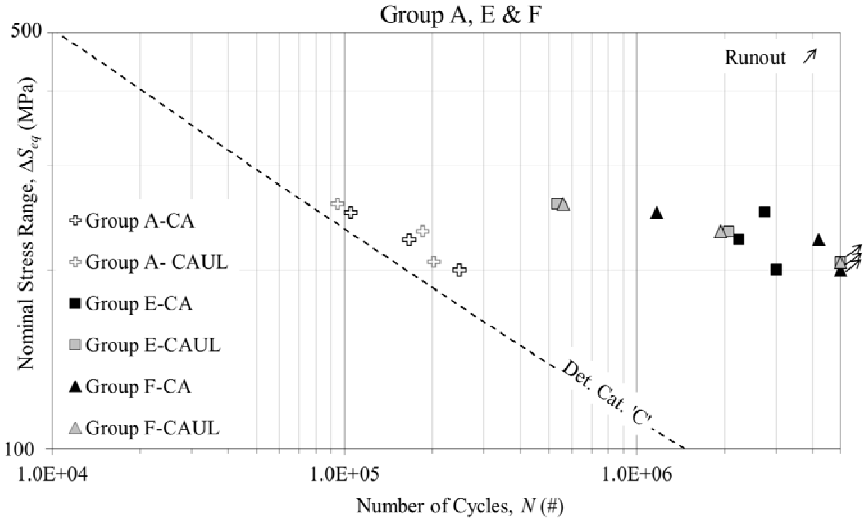

Figure 7 – Group A, E, and F S-N Data

Figure 8 shows the S-N data for Groups A, B, C, D, and F. Here again, it can be seen that a significant fatigue life increase results, even for the under- and over-treated specimens in Groups B, C, and D. Looking at this figure, it is difficult to assess whether or not the treatment level has a significant effect on the fatigue performance. In the next section, a statistical analysis of the test results is presented, in order to further address this question.

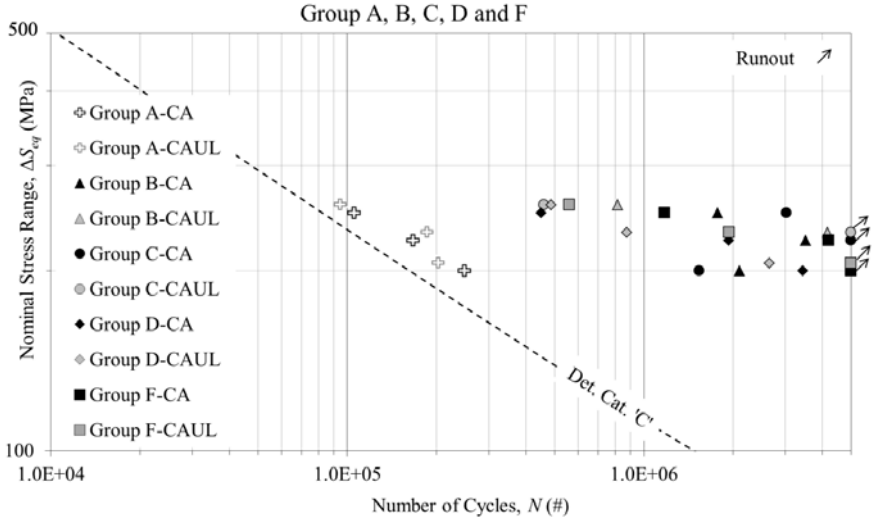

Figure 8 – Group A, B, C, D, and F S-N Data

For the Group G tests, a set of specimens were fatigue tested until the ACPD probes detected a crack depth of 0.5 mm. Following this, they were manually treated. In Figure 9, the results for this group are plotted. In this figure, the 'x' symbols show the load level and number of cycles

needed to pre-crack each specimen. The circular symbols show the fatigue life after treating. In general, a high degree of scatter is seen in these results. For two of the six tests, the lives are seen to be closer to the untreated specimen data. In general, these results confirm the importance of inspecting and, if necessary, repairing the weld before treatment.

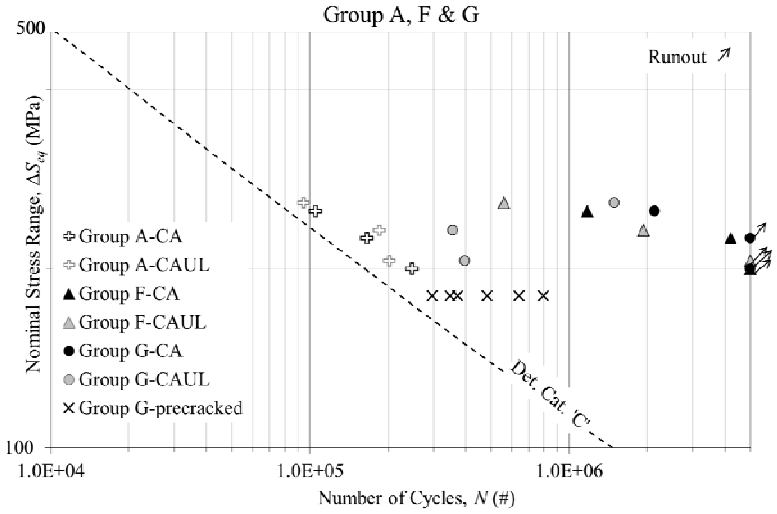

Figure 9 – Group A, F, and G S-N Data

Figure 10 shows crack growth curves, obtained using the ACPD technique, for Specimens A6 and F6. The effect of the treatment can be seen primarily at shallow crack depths (< 0.4 mm). At larger depths, the crack growth rate is similar for both specimens. In general, considerable "noise" was observed in the ACPD data. It is believed that this is a result of the magnetically attached probes vibrating excessively at the frequency of the cyclical loading. On this basis, no further analysis of this data was performed for the current study.

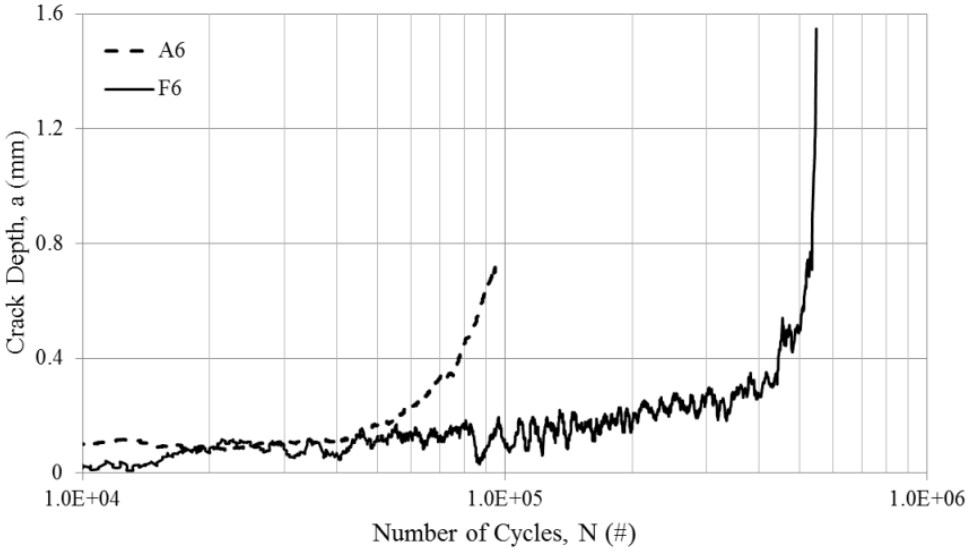

Figure 10 – Crack Growth Curves for Specimens A6 and F6

In order to investigate their use for quality control, weld toe geometry measurements such as the weld toe angle and radius before and after UIT application were obtained for each specimen. Sliced silicon impressions of the weld toe were placed under a microscope, and photographed. Measurements of the geometric parameters were then made using AutoCAD. The weld toe radius measurements after treatment are summarized in Table 4. With the exception of the properly treated weld toes, it was often difficult to define and measure a single toe radius due to the irregular shape of the weld toe. The radius corresponding with the greatest indent depth on the base metal side was recorded when multiple radii were present.

Table 4 – Statistical Results of Radius Measurements for Treated Specimens.

Group	Average (mm)	Std. Dev. (mm)
B	1.76	0.36
C	2.09	0.18
D	1.17	1.09
E	1.69	0.27
F	2.37	0.11

Indent depth measurements were taken with respect to a best fit line of the base metal surface. This is the conventional definition of indent depth, and is similar to the depth that weld inspectors measure to check for an undercut, when assessing weld quality. In addition, a best fit line was drawn along the surface of the weld, and a second indent depth was measured perpendicular to this line. Results of the two indent depth measurements are summarized in Tables 5 for the “base metal” side and Table 6 for the “weld” side.

Table 5 – Statistical Results of Indent Depth Measurements (Base Metal).

Group	Average (mm)	Std. Dev. (mm)	Maximum (mm)
B	0.16	0.04	0.19
C	0.16	0.06	0.22
D	0.17	0.15	0.39
E	0.36	0.40	1.10
F	0.27	0.07	0.37

Table 6 – Statistical Results of Indent Depth Measurements (Weld).

Group	Average (mm)	Std. Dev. (mm)	Maximum (mm)
B	0.51	0.28	0.79
C	0.37	0.16	0.61
D	1.10	0.27	1.43
E	0.53	0.38	0.92
F	0.25	0.14	0.51

The objective of the microhardness tests was to obtain the local material hardness at the weld toe of the untreated and treated specimens. For all of the specimens, eleven indentations were made along the expected crack path. These indentations started from 0.1 mm below the surface and then every 0.2 mm up to a depth of 2.1 mm. Each measurement set was repeated in three trials for each specimen. The measurements for the untreated specimen (Group A) were uniform with respect to depth below the surface and ranged from ~190-275 HVN. The envelopes for the treated specimens in Groups B-G are presented in Figures 11 and 12.

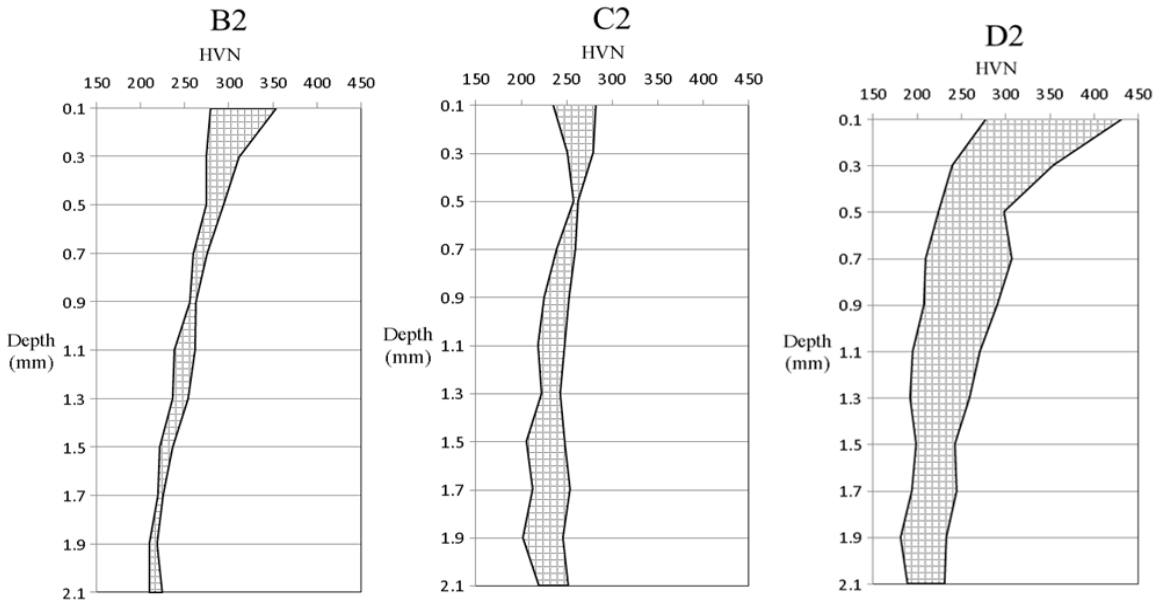

Figure 11 – Microhardness Measurements for Specimens B2, C2, and D2

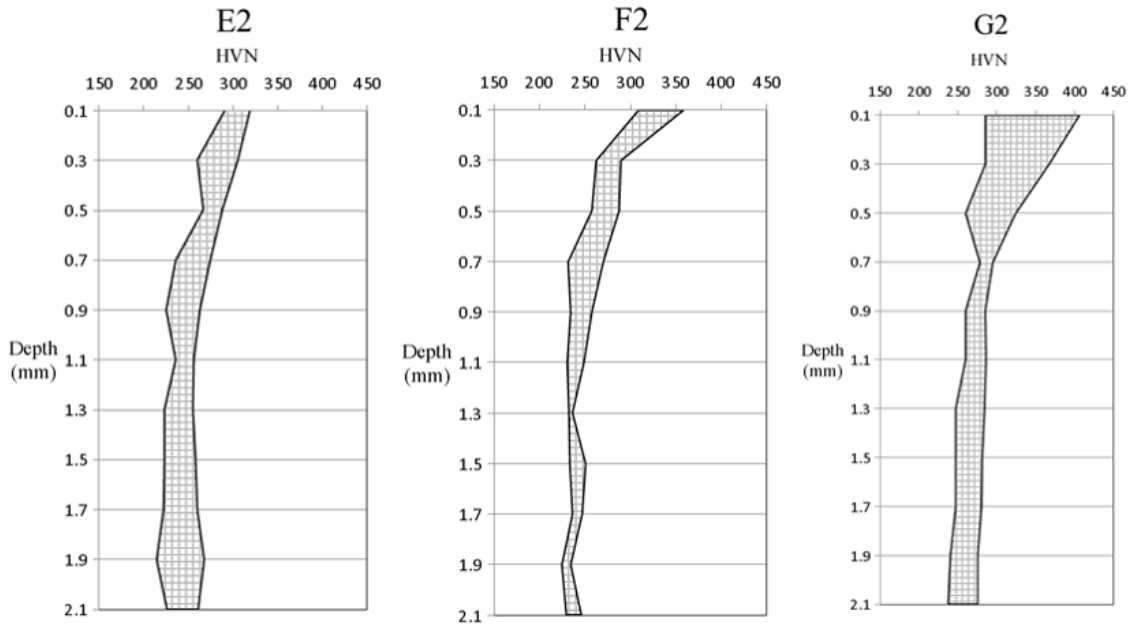

Figure 12 – Microhardness Measurements for Specimens E2, F2, and G2

The first measurement at 0.1 mm is normally the highest in the treated specimens. Below this, the HVN decreases with depth. In general, it is observed that the surface hardness is greatest for the over-treated group (D), followed by the properly treated groups (E, F, and G). Under-treating by reducing the treatment intensity (Group B), has little effect on the surface hardness. On the other hand, under-treating by increasing the treatment speed (Group C) does result in a decrease in the surface hardness to a level similar to the untreated group (A).

Residual stress measurements, obtained by Proto Manufacturing using the x-ray diffraction technique, are summarized in Table 7 and Figure 13. Measurements were taken on specimens after testing at depths of 0, 0.15, 0.3, 0.6, and 1.2 mm. In general, the measurements at depths 0 and 0.15 mm were highly erratic. A subsequent finite element analysis showed that the local stresses due to cyclic loading exceeded the static yield strength of the material at these depths, meaning that this material was likely deforming plastically with each load cycle, resulting in significant modification of the residual stresses at these depths. Looking at the measurements for depths of 0.3 to 1.2 mm, it can be seen that the residual stresses in the untreated specimen were already slightly compressive. It is believed that this was likely not the case for all of the untreated specimens, based on previous measurements reported by [Ghahremani 2010] for the same weld procedure and specimen geometry. For the treated specimens, the compressive stresses are highest in magnitude for the over-treated (Group D) specimen, followed by the properly, manually treated (Group F) specimen. The residual stress levels for the Group B and E specimens are similar. The residual stress magnitudes are much lower, however, for the Group C specimen, which was under-treated by increasing the treatment speed.

Table 7 – Residual Stress Measurements for Groups A-F.

Depth (mm)	Residual Stress (MPa)											
	A1		B1		C1		D1		E4		F1	
0.30	-110	± 7	-252	± 13	-81	± 7	-609	± 23	-241	± 7	-469	± 9
0.60	-90	± 8	-266	± 5	-114	± 9	-614	± 25	-254	± 2	-368	± 7
1.20	-119	± 6	-361	± 13	-214	± 16	-399	± 7	-360	± 9	-229	± 7
Average:	-106		-293		-136		-541		-285		-355	

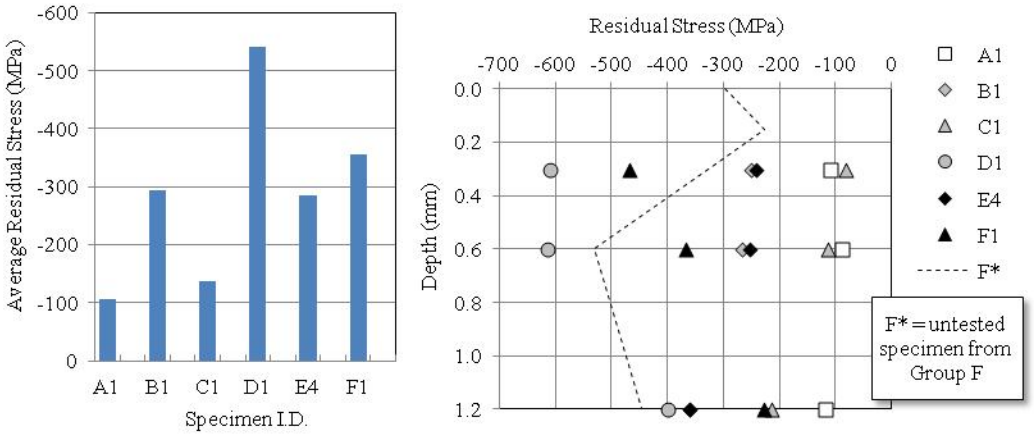

Figure 13 – Residual Stress Measurements for Groups A-F

Statistical Analysis of Fatigue Life Data

In order to establish design stress-life (S-N) curves for a specific survival probability with limited fatigue test data, a Gaussian log-normal distribution can be assumed. Ten or more failed test results (i.e. not run-outs) should be used if possible [Hobbacher, 2005]. For analyzing the fatigue data, a regression model is used where log(*N*) is the dependent variable. Characteristic values are calculated for *k* standard deviations of the dependent variable from the mean. These values correspond with a 95% survival probability with a two-sided 75% confidence level of the mean, according to the International Institute of Welding (IIW) Recommendation [Hobbacher, 2005]. Other standards, e.g. [AASHTO 2008b, CAN/CSA S6-06], use design curves based on a 97.7% survival probability, or two standard deviations below the mean.

Due to the limited test data available, a statistical analysis of the test data obtained for the current study was carried out with four different sets of assumptions, and denoted Cases I-IV. For Case I, run-out test results were included and the S-N curve slope, *m*, was fixed at 3.0, as is often assumed for steel. Case II is similar to Case I except that the run-out test results were removed. Case III includes run-outs and a variable *m*. Case IV does not include the run-out test results but does assume a variable *m*. To further increase the sample size for each statistical analysis, the test results for the treated specimens were grouped together in various ways. Groups B, C, and D were combined into a larger data set of specimens known to be "improperly treated". Groups E and F were combined into a data set of "properly treated" specimens. Groups B, C, D, E, and F were combined into a larger data set of specimens subjected to treatment, with the treatment quality "unknown". Figures 14-17 present results of the statistical analysis, in the form of calculated "mean" and "design" S-N curves for Cases I and IV.

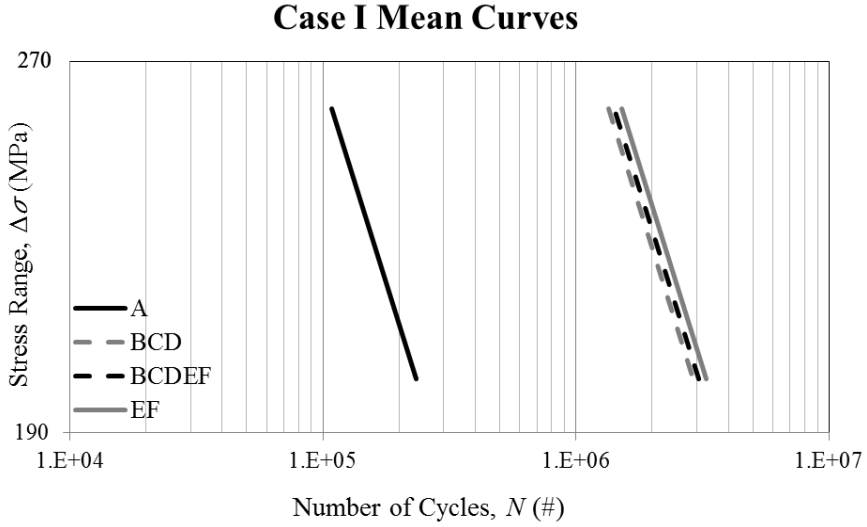

Figure 14 – Case I Mean Curves

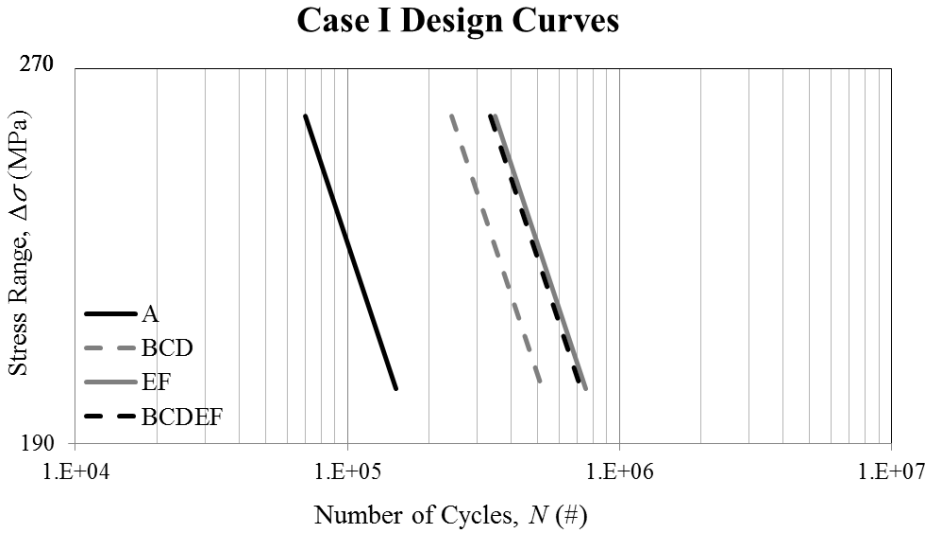

Figure 15 – Case I Design Curves

Looking at the results for the Case I analysis (run-outs included, $m = 3.0$), it can be seen that the mean curves for the treated specimens are shifted considerably to the right, indicating an increase in the mean fatigue life due to UIT (see Figure 14). The curves for the three different groups of treated specimens essentially fall on top of each other, however, suggesting that the effects of over- or under-treatment are minimal. Looking at the design curve results for the same case (Figure 15), the curves for the different groups of treated specimens are seen to be somewhat more dispersed. The curve for specimens known to be improperly treated (BCD) is the lowest, the one for properly treated specimens is the highest and the one for unknown treatment quality (BCDEF) falls in between. Similar trends are seen for Case IV (no run-outs, variable m) in Figures 16 and 17. In general, the same trends were seen regardless of whether or not run-outs were included in the analysis or whether m was fixed or variable.

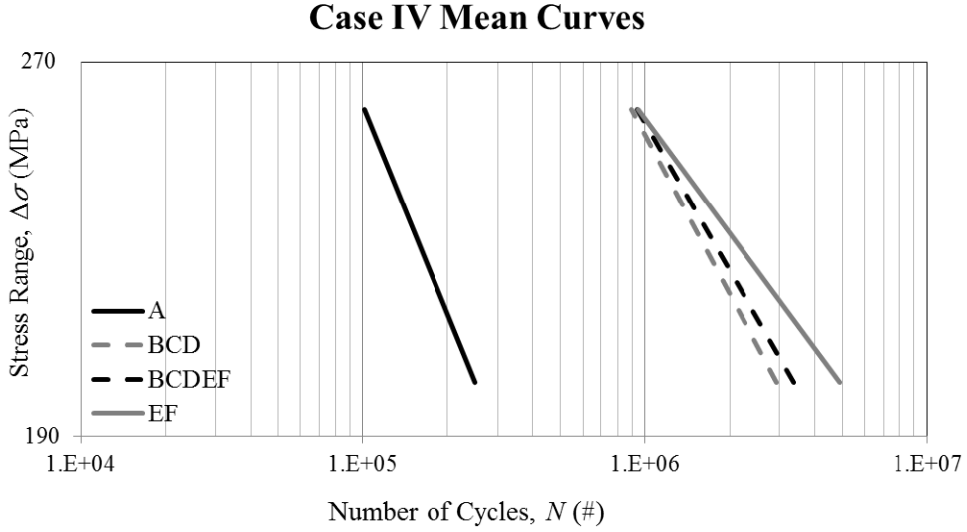

Figure 16 – Case IV Mean Curves

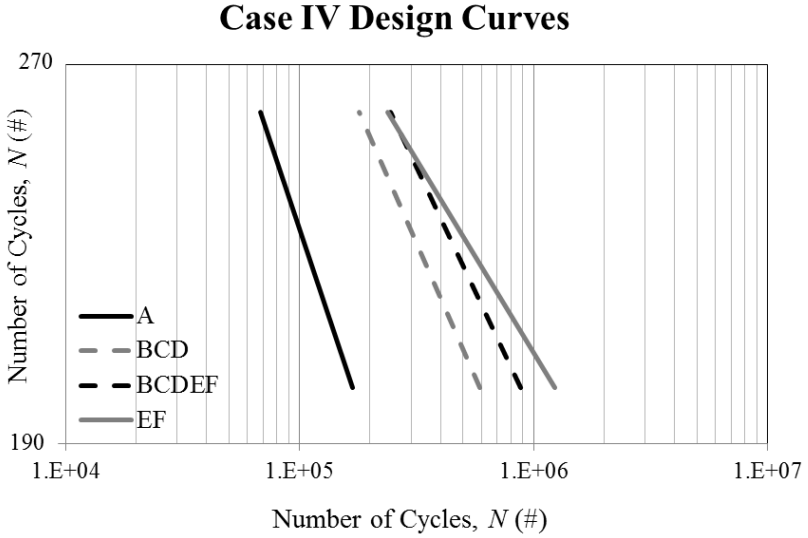

Figure 17 – Case IV Design Curves

Table 8 presents parameters define the mean and design curves for each of the four cases. In this table, m defines the slope and $\log_{10}(M)$ defines the vertical position, where:

$$\log_{10}(M) = m \cdot \log_{10}(\Delta S) + \log_{10}(N)$$

Table 8 – S-N Curve Parameters for Cases I-IV.

			Mean		Design	
		m	$\log_{10}(M)$	$\Delta S(2\cdot10^6)$	$\log_{10}(M)$	$\Delta S(2\cdot10^6)$
Case I	A	3.0	12.27	97.70	12.08	84.54
	BCD	3.0	13.37	226.53	12.62	127.58
	BCDEF	3.0	13.39	230.07	12.76	142.61
	EF	3.0	13.42	235.49	12.78	144.48
Case II	A	3.0	12.27	97.70	12.08	84.54
	BCD	3.0	13.27	210.13	12.55	121.04
	BCDEF	3.0	13.30	215.10	12.69	134.63
	EF	3.0	13.35	223.06	12.65	131.21
Case III	A	3.54	13.54	111.08	13.36	99.32
	BCD	5.41	19.05	227.03	18.34	167.85
	BCDEF	5.99	20.44	228.86	19.87	184.28
	EF	6.86	22.51	231.04	22.03	196.73
Case IV	A	3.54	13.54	111.08	13.36	99.32
	BCD	4.63	17.11	217.16	16.42	153.56
	BCDEF	5.00	18.04	222.02	17.45	169.80
	EF	6.41	21.43	229.88	20.83	185.31

An additional parameter, $\Delta S(2 \cdot 10^6)$, is also provided in Table 8. This is the stress range corresponding with a fatigue life of $N = 2 \cdot 10^6$ cycles – a parameter commonly used to describe the vertical position of the S-N curve, and also the "detail category", in various European standards and recommendations (e.g. [Hobbacher, 2005]). Comparing this parameter for the various data sets, the increase in fatigue strength due to UIT can be quantified.

When using UIT to extend the service life of an existing structure, it is the increase in fatigue life that is of interest. In order to quantify the benefit of treatment for the various levels of treatment quality, comparisons of fatigue life were made for a stress range of 200 MPa. Table 9 and 10 show the percent increases in fatigue life, based on the mean and design curves respectively. All of the comparisons are made with respect to the Curve A fatigue life. The percent increases in fatigue life based on the design curves are lower than those based on the mean curves. However, a similar trend is observed in terms of the ranking of each data set.

Table 9 – Fatigue Life Increase at ΔS = 200 MPa based on Mean Curves.

	% increase in fatigue life		
Mean	**BCD**	**BCDEF**	**EF**
Case I	1147%	1206%	1300%
Case II	895%	967%	1090%
Case III	1489%	1694%	2052%
Case IV	1071%	1249%	1853%
Average	1150%	1279%	1574%

Table 10 – Fatigue Life Increase at ΔS = 200 MPa based on Design Curves.

	% increase in fatigue life		
Design	**BCD**	**BCDEF**	**EF**
Case I	244%	380%	399%
Case II	194%	304%	274%
Case III	361%	628%	962%
Case IV	250%	424%	629%
Average	262%	434%	566%

In order to assess the significance of the trends observed in the fatigue test data, a set of t-test analyses were performed. The t-distribution is a bell-shaped and symmetric distribution with a zero mean, which is widely used in statistics. This distribution can be used for sample sizes less than thirty and its equations are derived from a normal population [Walpole & Myers, 1998]. The t-distribution can be used to compare data sets and determine whether or not their means are significantly different. In the t-test analyses carried out for this study, a two-sided test was used. In order to perform these analyses, the parameter, M, which is independent of the stress range, was calculated for each test results. A slope of $m = 3.0$ was used to calculate M.

Figure 18 shows a graph of the *M* vs. Δ*S*, illustrating the independence of *M* on Δ*S*.

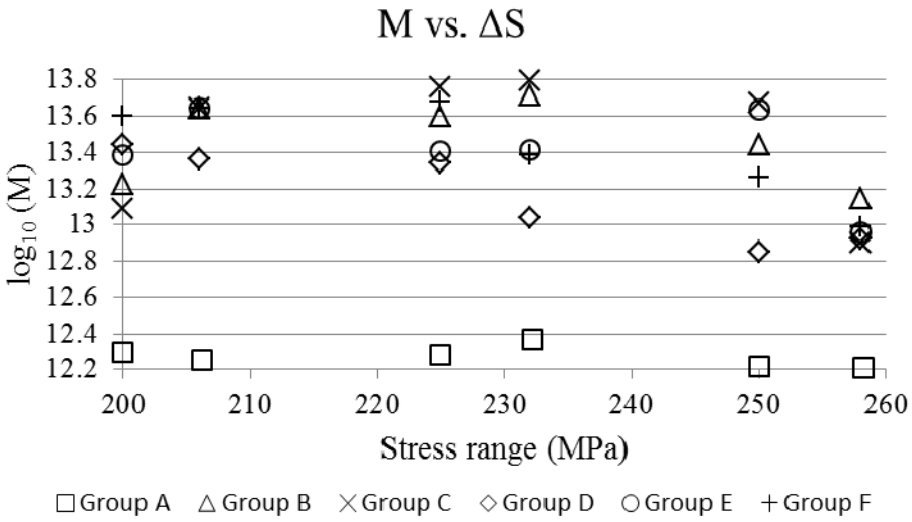

Figure 18 – *M* vs. Δ*S* Data for each Specimen Group.

Table 11 summarizes the results of the t-tests. In general, if the percentage in the second column of this table is below a pre-defined threshold (1 or 5% are commonly used), then it can be concluded that there is a significant difference between the data sets being compared. Looking at the results in this table, it can be seen that the probabilities obtained from comparing the Group A results with any of the treated groups, are extremely low. From this, it can be concluded that the fatigue life increase due to UIT is statistically significant, regardless of whether the specimens are under-, over-, or properly treated. The t-tests for the properly treated specimens (Group E) compared with the various under- and over-treated groups result in much higher percentages. From this, it can be concluded that the data sets are not large enough to confirm the statistically significance of observed differences in these data sets.

Table 11 – T-Distribution Results.

Data Sets Compared	Probability that data sets are from the same population
A vs. EF	$6.67 \cdot 10^{-9}$%
A vs. BCD	$1.76 \cdot 10^{-5}$%
A vs. BCDEF	$6.17 \cdot 10^{-11}$%
E vs. F	90%
E vs. B	70%
E vs. C	72%
E vs. D	12%
EF vs. BCD	65%

Finite Element Analysis

The finite element (FE) method was used in this research project to predict stress concentration factors (SCFs) along the crack path for the various treatment cases. In this context, the SCF is defined as the local elastic stress divided by the nominal, remotely applied stress. The nominal applied stress is taken as the applied load divided by the cross section area of the loaded plate. The ABAQUS CAE Version 6.11 software was used to perform the FE analysis. Sixteen specimens were chosen for modelling. To perform the FE analysis, a 2D plane strain model was chosen and the material properties were assumed to be homogenous and linear elastic. Nominal values of 200,000 MPa and 0.3 were assigned as the Young's modulus (E) and Poisson's ratio (μ) respectively. A 1.0 mm node spacing was used in the regions of the specimen far removed from the weld toe. At the weld toe, a much smaller node spacing of 0.02 mm was prescribed. The meshed model of Specimen F1 is shown below in Figure 19.

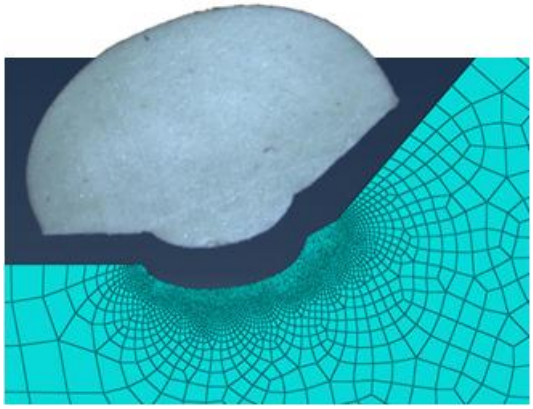

Figure 19 – Specimen F1 Weld Toe 1 Impression and FE Mesh

Table 11 presents the stress concentration factors (SCFs) for the analyzed specimens.

Table 11 – Peak Stress Concentration Factors (SCFs).

		After Treatment				Thickness Study		
Group	Before Treatment	1	2	3	Average	19 mm	38 mm	75 mm
A	(A1) 2.76	-	-	-	-	-	-	-
B	(B1) 2.73	(B1) 2.15	(B3) 1.96	(B5) 1.96	2.02	(B3) 2.13	(B3) 2.18	(B3) 2.17
C	(C1) 2.37	(C1) 2.03	(C3) 1.87	(C5) 2.20	2.03	-	-	-
D	(D1) 2.67	(D1) 2.68	(D4) 2.86	(D6) 3.14	2.82	(D6) 3.31	(D6) 3.37	(D6) 3.37
E	(E1) 3.49	(E1) 1.95	(E3) 2.06	(E6) 2.25	2.09	(E3) 2.28	(E3) 2.33	(E3) 2.32
F	(F1) 3.89	(F1) 1.86	(F4) 2.29	(F6) 2.21	2.12	-	-	-
G	-	(G1) 2.13	-	-	-	-	-	-

In Table 11, the ID of the specimen from which the weld toe impression was taken is placed before the SCF in brackets. For each treatment case, three weld toes were analyzed. Six untreated weld toes were also analyzed. In order to study the effect of plate thickness on the SCF, three of the treated specimen models were modified after the initial analysis by increasing the plate thickness from $T = 9.5$ mm (the actual thickness) to 19, 38, or 75 mm.

Looking at Table 11, it can be seen that the SCFs are generally higher before treatment. The average peak SCF for the six analyzed as-received welds was 2.99. Proper treatment reduces the peak SCF to 2.09 (robotic treatment) or 2.12 (manual treatment). Under-treatment results in a similar or slightly greater reduction in the SCF, while over-treatment results in a peak SCF that is almost as large as the average value for the as-received welds.

The results of the thickness study presented in Table 11 show that the peak SCF increases with an increase in the plate thickness. This result is not unexpected, since as the plate thickness increases, the ratio of the plate thickness to the weld toe radius also increases, resulting in a similar effect to increasing the sharpness of the notch. In general, the peak SCFs were seen to stabilize for plate thicknesses, T, greater than 38 mm.

Figures 20 to 22 show SCF distributions through the plate thickness (along the anticipated crack path), for a number of the analyzed weld toes. In Figure 20, the untreated and properly treated SCF distributions are compared. Both the manual and robotic treatment processes can be seen to result in a significant SCF reduction near the surface. In Figure 21, the SCFs for the under- and over-treated specimens are plotted. Importantly, it can be seen in this figure that the SCF at the surface for the over-treated specimen (D1) is similar to that of an untreated weld.

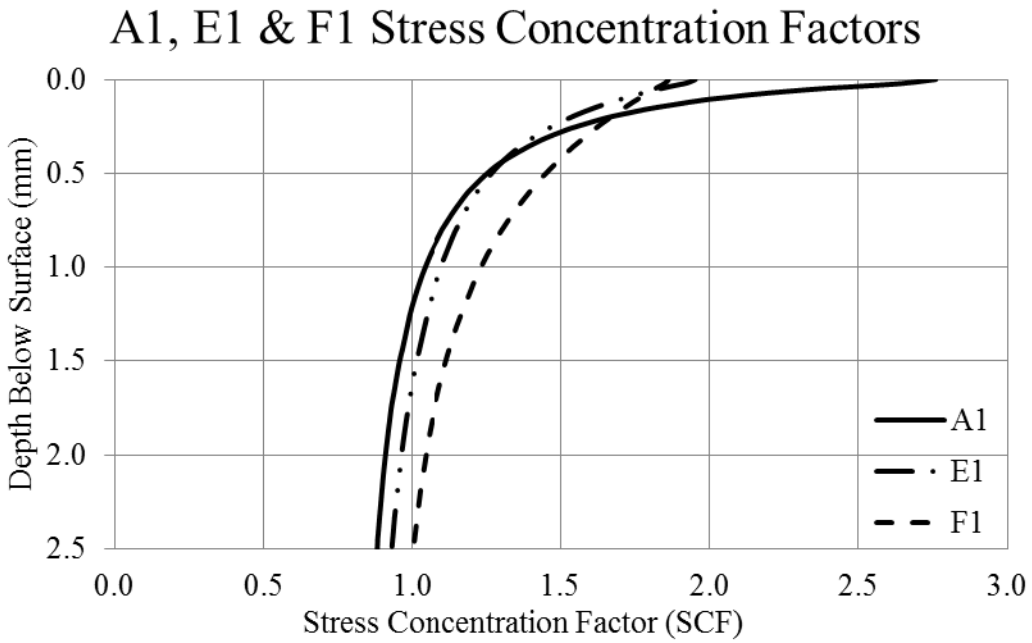

Figure 20 – SCF Results for Untreated and Properly Treated Specimens

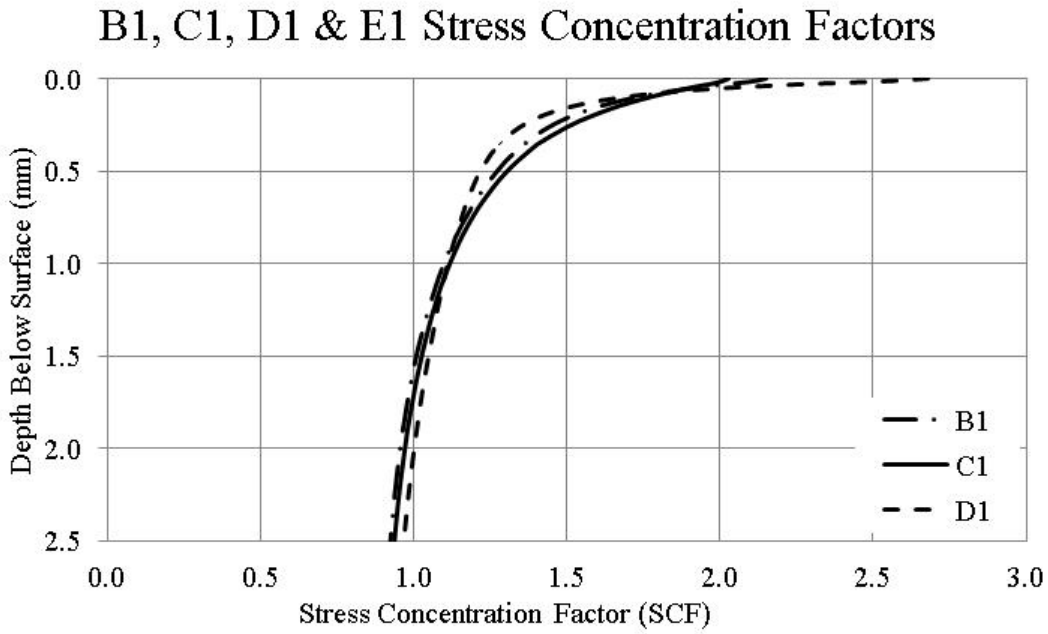

Figure 21 – SCF Results for Under- and Over-Treated Specimens

In Figure 22, sample results of the plate thickness study are presented for Specimen E3. Looking at this figure, it can be seen that the SCFs increase with an increase in plate thickness, but stabilize for $T > 38$ mm. This trend was typical for all of the analyzed weld toes.

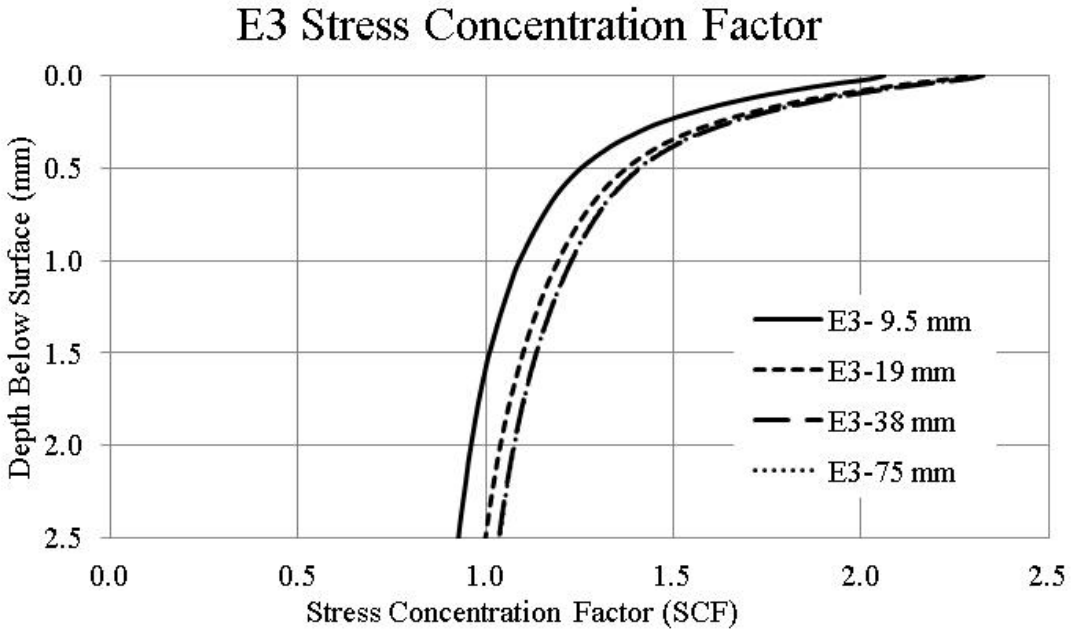

Figure 22 – E3 SCF Results for Various Plate Thicknesses

Analysis of Indent Depth Measurements

Indent depth is useful and recognized parameter for the quality control of residual stress-based post-weld treatments such as UIT, due to the ease with which it can be obtained and the strong correlation that it appears to have with treatment quality. Figure 23 shows the base metal indent depth measurements for all the treated groups (i.e. the indent depth measurements taken with respect to the base metal surface). As stated earlier, these measurements were obtained by taking photographs of silicon impressions and measuring the distance to the bottom of the notch, perpendicular to a best fit line drawn along the original surface.

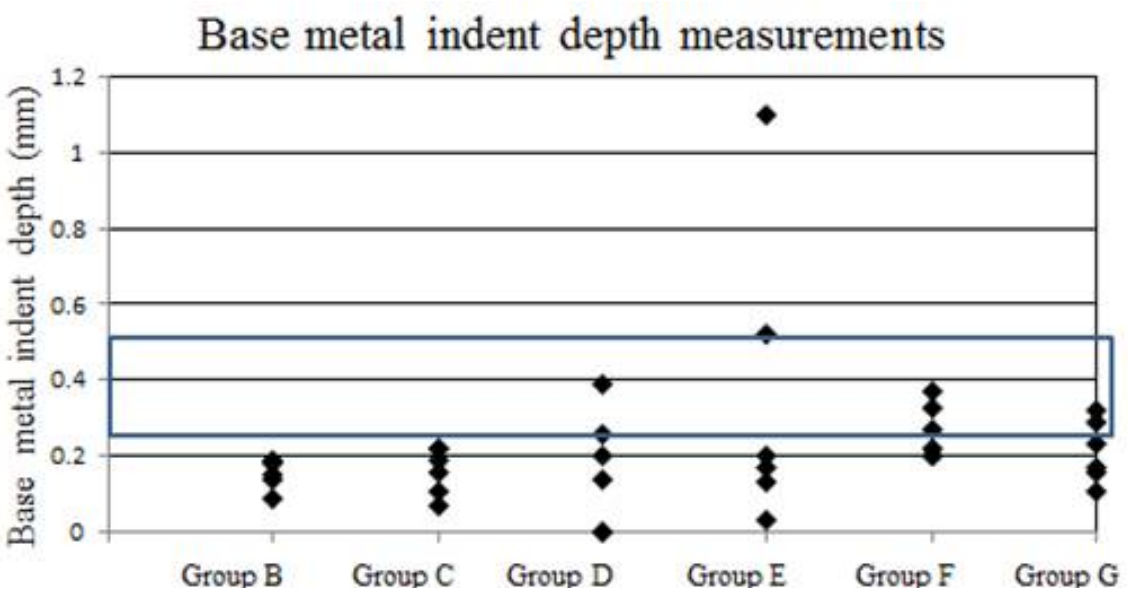

Figure 23 – Indent Depth: Measurements from Base Metal Side

The rectangular region in Figure 23 denotes the acceptable indent depth range for UIT recommended by [AASHTO 2008a], which is 0.25-0.5 mm. In general, it was observed that for the robotic treatment, the tool was directed to a much larger degree towards the weld, rather than the base metal. Hence, the indent depths for the base metal were lower than expected for the robotically treated Groups. However, the manually treated specimens in Groups F and G fall within or close to the identified standard range. Figure 24 shows the average of the base metal and weld indent depth measurements for all of the treated groups.

Using the average indent depth, based on measurements of a weld toe impression, it is easier to identify that the specimens in Group D are over-treated. On the other-hand, while the average indent depths for the undertreated specimens fall below those for the specimens treated properly using the same robotic process, the indent depths for the specimens undertreated robotically are similar to those for the specimens treated properly using the manual process. A similar trend can be seen in the maximum indent depth results in Figure 25.

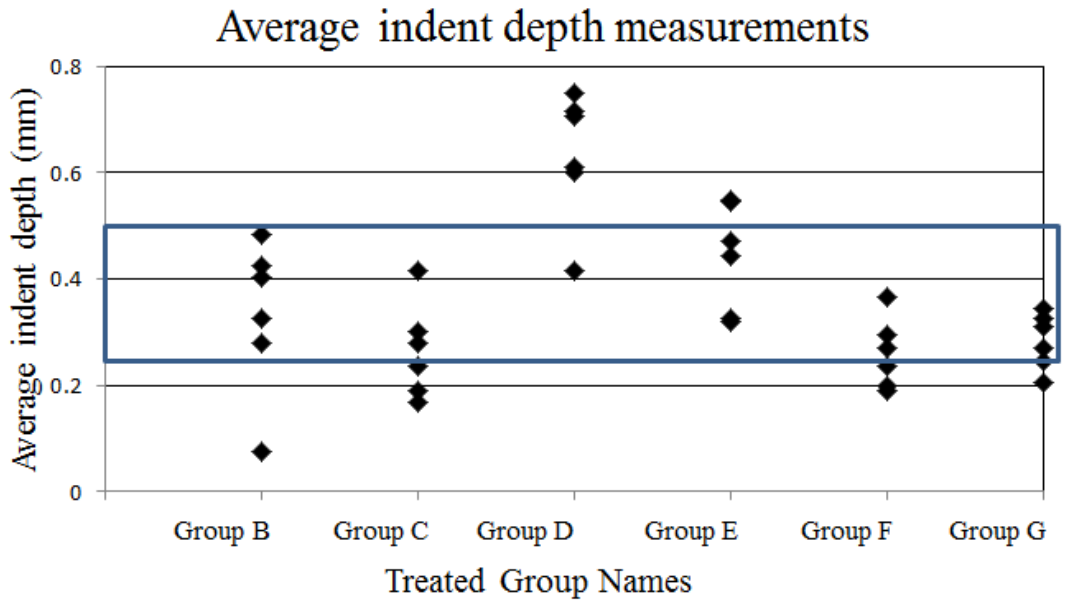

Figure 24 – Indent Depth: Average of Base Metal and Weld Measurements

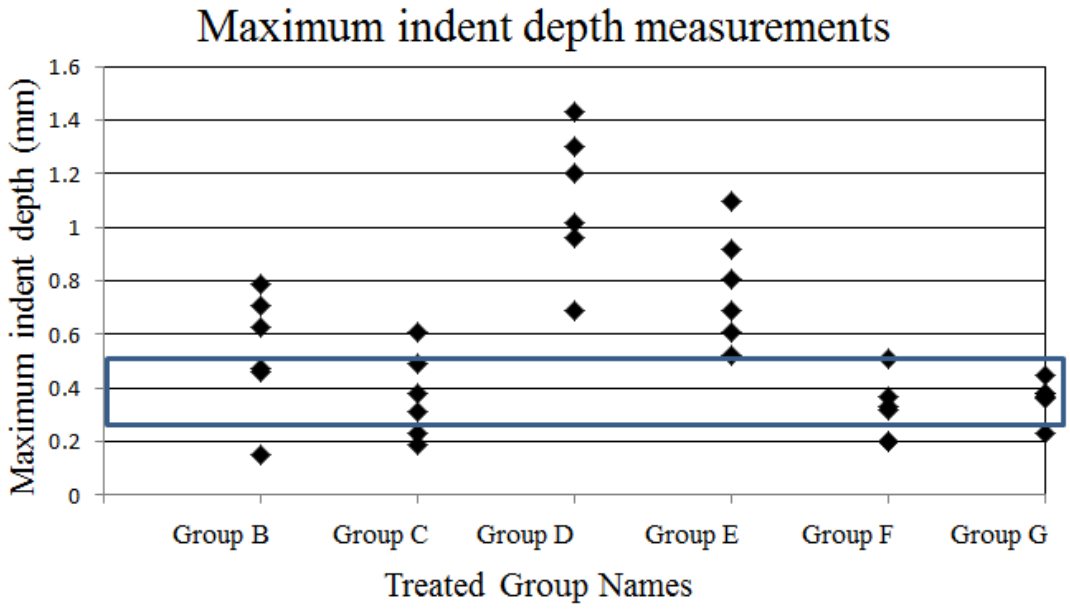

Figure 25 – Indent Depth: Maximum of Base Metal and Weld Measurements

Based on these results, it is concluded that the indent depth is a good parameter for quality control, and in particular for identifying over-treatment. Since the data for the under-treated specimens are very similar to the data for the manually treated specimens, it is recommended to perform a precise and accurate visual inspection of the weld toe in addition to the indent depth measurements, to identify if a weld has been under-treated. When visually inspecting for under-treatment, the goal should be to ensure that any evidence of the original weld toe, similar to the line running along the treated region in Figure 5(bottom right), is avoided.

Conclusions

The main conclusions of this study can be summarized as follows:

- Ultrasonic impact treatment (UIT) resulted in a significant increase in the fatigue life of the welded steel specimens, regardless of the simulated level of treatment "quality". Manually or robotically treating the specimens resulted in a similar performance in terms of increasing the fatigue life. On average, the fatigue lives of the treated specimens were slightly lower when there were under-loads in the loading history.

- The simulated level of treatment quality had little impact on the mean S-N curve. Treatment quality did have an impact, however, on the design (95% survival probability) S-N curves, with the curve associated with "proper treatment" slightly higher than the curves for poor or unknown treatment quality.

- The near-surface microhardness and compressive residual stresses are greatest for the over-treated specimens, followed by the properly treated specimens. UIT resulted in a significant change in the residual stress distribution through the plate thickness. Increasing the treatment speed results in a greater reduction in the surface microhardness and compressive residual stresses than decreasing the treatment intensity.

- Finite element (FE) analyses show that the change in weld toe geometry due to UIT can cause a significant decrease in the stress concentration factor near the surface of the treated weld toe. The stress concentration factors were lowest for the properly treated specimens and slightly higher for the under-treated specimens. For the over-treated specimens, the stress concentration factors were nearly as high as for untreated welds. The FE analyses also showed that as the plate thickness increases, the SCF increases as well, up to a thickness of $T = 38$ mm, beyond which there is no substantial change in the SCF.

- Indent depth measurements from the base metal side, commonly used for quality control, may not identify over-treatment on their own, if the UIT tool is directed primarily at the weld metal. Indent depth measurements from both the weld and the base metal side, obtained using weld toe impressions, offer a good alternative means for identifying over-treatment. For identifying under-treatment, indent depth measurements should be used in conjunction with visual inspection for traces of the original weld toe.

Recommendations

Based on the experiments done and results obtained in this research study, the following recommendations are made, with regards to the quality control of UIT:

- The current recommendations for the visual inspection of welds treated by UIT, for example in [AASHTO 2008a] ,would have likely been successful in identifying the under- and over-treated weld specimens fabricated for the current study.

- For identifying over-treatment, indent depth measurements from both the weld and base metal sides, obtained by measurement of weld toe impressions, are recommended as a means of further verifying the treatment quality. Evidence of significant flaking as a result of the treatment is another practical means for identifying over-treatment, if the inspector is present during the treatment. For identifying under-treatment, indent depth measurements should be used in conjunction with visual inspection for traces of the original weld toe.

- Through-thickness microhardness and residual stress measurements are not practical for application to actual structures, since they require destruction of the weld. However, strong correlations were seen between these parameters and the simulated level of treatment quality. On this basis, the use of these methods on sample specimens is recommended, for the evaluation of new UIT methods or procedures.

Acknowledgements

The Ministry of Transportation of Ontario (MTO) is gratefully acknowledged for providing financial support for this research. MTO engineers Bala Tharmabala, Clifford Lam, and Ranko Mihaljevic are also thanked and acknowledged for their technical indput.

Applied Ultrasonics is gratefully acknowledged for providing specimen treatment. Sam Abston at Applied Ultrasonics is thanked in particular for his technical input.

At the University of Waterloo, technical support for this research was provided by Richard Morrison, Doug Hirst, and Rob Sluban. Assistance in the laboratory was also provided by Kasra Ghahremani and Iris Chang. In addition, the master's thesis, on which this report is based, was reviewed and improved based on comments provided by Profs. Tim Topper and Monica Emelko. These individuals are thanked for their contribution to this work.

References

AASHTO. (2008a). American Association of State Highway and Transportation Officials: LRFD Bridge Construction Specifications, Interim Revisions. Washington, D.C.

AASHTO. (2008b). American Association of State Highway and Transportation Officials: LFRD bridge design specifications. (4th Ed.). Washington, D.C.

American Welding Society (AWS). (2004). Structural Welding Code. AWS Standard D1.1/D1.1M.

Canadian Standards Association (CSA). (2003). Welded Steel Construction (Metal Arc Welding). CSA Standard W59-03.

Canadian Standards Association (CSA). (2006). Canadian highway bridge design code CAN/CSA-S6-06.

Cheng, X., Fisher, J.W., Prask, H.J., Gnäupel-Herold, T., Yen, B.T., & Roy, S. (2003). Residual stress modification by post-weld treatment and its beneficial effect on fatigue strength of welded structures. International Journal of Fatigue, 25:9-11, 1259-1269.

Costa Borges, L. A. (2008). Size effects in the fatigue behaviour of tubular bridge joints. EPFL, Lausanne, Switzerland. Thesis No. 4142.

Det Norske Veritas (DNV). (2001). Fatigue Strength Analysis of Offshore Steel Structures. DNV Recommended Practice RP-C203.

Ghahremani, K. (2010). Predicting the effectiveness of post-weld treatments applied under load. (Master of Applied Science, University of Waterloo). 129.

Gunther, H.-P., Kuhlmann, U., & Durr, A. (2005). Rehabilitation of Welded Joints by Ultrasonic Impact Treatment (UIT). IABSE Symposium, Lisbon.

Haagensen, P. J., Statnikov, E. S., & Lopez-Martinez, L. (1998). Introductory fatigue tests on welded joints in high strength steel and aluminium improved by various methods including ultrasonic impact treatment (UIT). International Institute of Welding, Doc. XIII-1748-98

Haagensen, P.J. & Maddox, S.J. (2000). IIW Recommendations on the Post Weld Improvement of Steel and Aluminum Structures. International Institute of Welding, Doc. XIII-1815-00.

Hobbacher, A. (2005). Recommendations for fatigue design of welded joints and component. International Institute of Welding, Doc. XIII-1965-03/XV-1127-03.

Kuhlmann, U., Durr, A., & Gunther, H.-P. (2006). Application of post-weld treatment methods to improve the fatigue strength of high strength steels in bridges. IABMAS-06, Porto.

Lugg, M. C. (2008). TSC Inspection Systems.

Nyborg, E., Moffatt, P., Cavaco, J., & Nyborg, D. (2006). Ultrasonic impact treatment for life extension of bridges with crack and crack susceptible welded details. IAMBAS-06, Porto.

Roy, S. (2006). Experimental and Analytical Evaluation of Enhancement in Fatigue Resistance of Welded Details Subjected to Post-Weld Ultrasonic Impact Treatment. Doctoral Thesis, Department of Civil and Environmental Engineering, Lehigh University.

Roy, S., Fisher, J.W., & Yen, B.T. (2003). Fatigue resistance of welded details enhanced by ultrasonic impact treatment (UIT). International Journal of Fatigue, 25:9-11, 1239-1247.

Ummenhofer, T., Weich, I., & Nitchke-Pagel, T. (2006). Fatigue life improvement of existing steel bridges. IABMAS-06, Porto.

Vilhauer, B., Bennett, C. R., Matamoros, A. B., & Rolfe, S. T. (2012). Fatigue behavior of welded coverplates treated with ultrasonic impact treatment and bolting. Engineering Structures, 34, 163-172.

Walpole, R. E. & Myers, R. H. (1998). Probability and statistics for engineers and scientists (6th Edition). New York: London: Macmillan; Collier Macmillan.